Mpelasoka, F. and Awange, J. and Zerihun, A. 2018. Influence of coupled ocean-atmosphere phenomena on the Greater Horn of Africa droughts and their implications. Science of the Total Environment. 610-611: pp. 691-702.

Influence of coupled ocean-atmosphere phenomena on the Greater Horn of Africa droughts and their implications

Freddie Mpelasoka[1], Joseph L. Awange[2], Ayalsew Zerihun[3]

[1]Hydrometeorology Independent Researcher, Canberra, Australia
[2]Department of Spatial Sciences, Curtin University, Perth, Australia
[3]Centre for Crop and Disease Management, Department of Environment and Agriculture, Curtin University, Perth, Australia

Abstract

Drought-like humanitarian crises in the Greater Horn of Africa (GHA) are increasing despite recent progress in drought monitoring and prediction efforts. Notwithstanding these efforts, there remain challenges stemming from uncertainty in drought prediction, and the inflexibility and limited buffering capacity of the recurrently impacted systems. The complexity of the interactions of ENSO, IOD, IPO and NAO, arguably remains the main source of uncertainty in drought prediction. To develop practical drought risk parameters that potentially can guide investment strategies and risk-informed planning, this study quantifies, drought characteristics that underpin drought impacts management. Drought characteristics that include probability of drought-year occurrences, durations, areal-extent and their trends over 11 decades (1903-2012) were derived from the Standardized Precipitation Index (SPI).Transient probability of drought-year occurrences, modelled on Beta distribution, across the region ranges from 10 to 40%, although most fall within 20-30%. For more than half of the drought events, durations of up to 4, 7, 14 and 24 months for the 3-, 6-, 12- and 24-month timescales were evident, while 1 out of 10 events persisted for up to 18 months for the short timescales, and up to 36 months or more for the long timescales. Apparently, only drought areal-extent showed statistically significant trends of up to 3%, 1%, 3.7%, 2.4%, 0.7%, -0.3% and -0.6% per decade over Sudan, Eritrea, Ethiopia, Somalia, Kenya, Uganda and Tanzania, respectively. Since there is no evidence of significant changes in drought characteristics, the peculiarity of drought-like crises in the GHA can be attributed (at least in part) to unaccounted for systematic rainfall reduction. This highlights the importance of distinguishing drought impacts from those associated with new levels of aridity. In principle drought is a temporary phenomenon while aridity is permanent, a deference that managers and decision-makers should be more aware.

Keywords: Drought; Greater Horn of Africa; Climate variability; Climate shift; Drought management; Drought related humanitarian crisis.

1. Introduction

The Greater Horn of Africa (GHA) shares many common experiences with the rest of the world when it comes to impacts of drought. However, the impacts of drought in some Member States of the GHA region often appear to have more adverse effects on sustainable development than elsewhere in similar developing countries (Venton, 2012). For example, for the southern Africa region, drought in Botswana is regarded as a learning opportunity to improve/achieve water security (UN, 2017). But for the GHA region, rather than responding successfully to the frequent recurrent droughts that afflict the region, the communities are invariably devastated by famine crisis, instabilities in national economies and political tensions. For example, the Ethiopian “biblical” famines of 1973-74 and 1984-85 left about 200,000 and 400,000, people dead, respectively, with the former disaster resulting in the overthrow of Emperor Haile Selassie (Baroody, 1995, Jansson et al., 1987). The latter contributed to the end of the Marxist regime of Mengistu Haile Mariam (LAT, 1991).

Nicholson (2014) describes the relatively recent drought related crisis in the GHA region that prevailed during much of the period 2008–2011 triggering extreme food shortages and massive migration. Currently, parts of GHA are in the midst of a major drought (IGAD, 2017). The most affected areas include most of Somalia, south-eastern Ethiopia, north-eastern and coastal Kenya, and northern Uganda, with Somalia and parts of Kenya facing severe famine. It is increasingly alarming that being in dire need of food assistance in the GHA is becoming a permanent feature of the region. Almost every year, including 2014, 2015, 2016 and 2017 famine headlines appear in the news as drought related crisis (FAO, 2017).

While droughts may continue to be a major problem, for some regions of the GHA, other factors such as armed conflicts and international politics, are invariably responsible for propelling a situation of economic hardship caused by droughts (FAO, 2007). For example, on a long-term basis, environmental degradation, poor water resource management and poor governance are important compounding causes of severe drought impacts in the region (UN, 2014). More importantly, aridity reconstruction studies (Tierney et al., 2015) show that the region is increasingly becoming drier. This systematic persistent decline in rainfall, particularly during much of the region’s primary rainy season (March-April-May) is evident in the last 30 years rainfall record (Williams and Funk, 2011, Lyon and DeWitt, 2012). Whether this decline trend is associated with internal multi-decadal climate variability due to changes in the tropical Pacific (Yang et al., 2014, Lyon and DeWitt, 2012) or anthropogenically driven warming in the Indian Ocean or western Pacific region (Liebmann et al., 2014), its impacts are yet to be distinguished from those associated with droughts. The impact of changes in aridity levels is often hardly distinguished from that of droughts. Drought is a recurrent feature of climate variability that occurs in virtually all climate regimes, and is different from aridity which is a rather permanent feature (Mpelasoka et al., 2008). Similarly, as underlying impoverishment of population increases, it is increasingly more difficult to distinguish between humanitarian crises triggered by drought impact and those stemming from chronic poverty (FAO, 2007).

Indeed, there are still many challenges in monitoring and prediction capabilities, as well as a perspective of the current understanding of drought and key research gaps. For example, almost all drought studies reiterate the influence of ENSO phenomenon on drought occurrences, with respect to drought prediction. However, there are other important ocean-atmosphere phenomenon. Such as the Indian Ocean Dipole (IOD), Inter-decadal Oscillation (IPO) and the North Atlantic Oscillation (NAO). The main challenge is to account for the interactions of different systems of climate variability and their teleconnections (Swetnam and Betancourt, 1998, Cook et al., 1999 , Cordery and McCall, 2000, Murphy and Timbal, 2008). The overall influence of climate variability drivers depends on their concurrent modes (Behera et al., 2006). Hence, this is the main source of uncertainty in predictions of climatic extremes including droughts particularly, when they are solely based on ENSO phenomenon (Kane, 1997). In addition to limited prediction skill, possibly the lack of flexibility in the impacted systems for the GHA underscore the effect of prediction. For example, currently, in Somalia and coastal Kenya cropping lands, 70% to 100% crop failure has been registered (IGAD, 2017). Livestock mortality has been particularly devastating amongst small ruminants with mortality rate ranging from 25% to 75% in the cross border areas of Somalia-Kenya-Ethiopia. This is happening regardless of early warnings by the Inter-Governmental Authority on Development, potentially meant to elicit early actions (preparedness and mitigation measures). Apparently, moving from crisis to risk management in the GHA requires planning that places more weight on risk assessment and the development and implementation of mitigation actions and programs as suggested in Wilhite et al. (2000).

This study has three main objectives: (1) quantification of the variation of influence among climate variability drivers across the region; (2) quantification of drought characteristics that underpin drought impacts management; and (3) examination of consistence of current increase in drought-like crises with trends in drought characteristics over the GHA region; The analyses include: (i) relating drought occurrences with climate variability drivers; (ii) modelling of transient probability of drought-year occurrences; (iii) determining drought duration; (iv) determining drought areal-extent; and (v) examining trends in rainfall.

2. Data and Methodology

2.1 Data

Monthly rainfall for the 1901-2013 period on a $0.1^o \times 0.1^o$ grid across the GHA region were drawn from the Centennial Trends Greater Horn of Africa precipitation dataset

(Funk et al., 2015). The CenTrends data set provides a reasonably complete and accurate gridded precipitation products.

Sea Surface Temperatures (SSTs) drawn from the NCEP/NCAR Reanalysis dataset (Kalnay et al., 1996) for the 1948-2013 period were used. The SSTs were used to derive indices of four major climate variability drivers that include the Oceanic Niño *Index* (*ONI*), which represents the El Niño Southern Oscillation (ENSO), Indian Ocean Dipole (IOD), Inter-decadal Pacific Oscillation (IPO) and the Northern Atlantic Oscillation (NAO).

2.2 Methodology

2.2.1 Identification of Drought events

Monthly rainfall time series were transformed into the Standardized Precipitation Index (SPI), developed by McKee et al. (1993) to capture rainfall variability from which occurrences of drought events were unveiled for the 1903 April – 2013 March period. The SPI is a probability index that gives a good representation of rainfall variability, quantifying abnormal wetness and dryness levels. Mathematically, the SPI is based on the cumulative probability of a given rainfall event occurring at a location. The historic rainfall data of the location is fitted to a gamma distribution, as the gamma distribution fits the precipitation distribution quite well. The cumulative probability gamma function subsequently transformed into a standard normal random variable. For comparison purposes, the World Meteorological Organization (WMO) recommends the use of SPI in monitoring of dry spells (WMO, 2012).

Since much of rainfall is experienced in short rainy seasons and most of it often concentrates in a few heavy falls, small shifts in the large-scale weather patterns at different timescales significantly alter the amount and/or the distribution of rainfall. Therefore, we use SPI at four timescales to facilitate the interpretation and relevance of rainfall anomalies to different systems. For this study, we focused on the 3-month, 6-month, 12-month and 24-month timescales, which are generally relevant to a range of agricultural and hydrological systems. For a given timescale, a drought event begins any time when the SPI is continuously less than negative 0.9 for at least 3 months, and ends when the SPI becomes greater than negative 0.9. This value is the threshold for dry conditions in the SPI classification, which is equivalent to 0.18 cumulative probability (McKee et al., 1993).

2.2.2 Modelling the probability of drought-year occurrences

Since the occurrences of a drought-year (derived from the SPI time series) are statistically independent in that there is no contribution of antecedent conditions, the modelling of transient probabilities of drought-year occurrences is rather straightforward.

The series of hits and misses of drought-year occurrences form proportions that can be represented with a *Binomial* or *Geometric* distribution with parameter p (Johnson et al., 1995, Weil, 1970). However, in practice these portions exhibit extra variations that cannot be explained by a simple *Binomial* or *Geometric* distribution because the parameter p does not remain constant in the course of time (Williams, 1975, Otake and Prentice, 1984). For the parameter p to assume a continuous distribution in the parameter space $0 < p < 1$, the best way is to follow the *Beta* distribution (Gupta and Nadarajah, 2004).

Beta distribution is a natural conjugate prior distribution in the Bayesian sense (i.e., evidence about the true state) and represents all possible values of unknown probabilities. Suppose these probabilities constitute a continuous random variable X that follow a *Beta* distribution with parameters α and β, where $0 < \alpha < 1$ and $0 < \beta < 1$; α and β are chosen to reflect any existing information/belief, then the probability density function of X takes the form of Equation 1.1 (Evans et al., 2000),

$$f(x \mid \alpha, \beta) = \frac{x^{\alpha-1}(1-x)^{\beta-1}}{\mathrm{B}(\alpha,\beta)}, \qquad 0 < x < 1, \tag{1.1}$$

where $\mathrm{B}(\alpha,\beta) = \frac{\Gamma(\alpha)\Gamma(\beta)}{\Gamma(\alpha+\beta)}$ is the beta function (acting as a normalizing constant) and where $\Gamma(\alpha)$ is the gamma function:

$$\Gamma(\alpha) = \int_0^\infty x^{\alpha-1} e^{-x} dx. \tag{1.2}$$

The mean and variance of the Beta random variable X are

$$\mu = \frac{\alpha}{\alpha+\beta}, \tag{1.3}$$

and

$$\sigma^2 = \frac{\alpha\beta}{(\alpha+\beta)^2(\alpha+\beta+1)}, \tag{1.4}$$

respectively.

Intuitively, the Beta distribution is particularly attractive for modelling the dynamics of the probability of drought-year occurrences, as more information become available. If h and m are numbers of hits and misses of drought-year occurrences respectively, at the i^{th} time step, while the mathematics for proving the updating procedure is a bit involved, the operation is very simple. The *Beta* distribution takes the form of Equation 1.5 (Evans et al., 2000).

$$Beta(\alpha_i, \beta_i) = Beta(\alpha_{i-1} + h, \beta_{i-1} + m) \quad (1.5)$$

For each grid-cell, the initial parameters *α*, *β* were estimated from a *prior probability* based on the proportion count of years in drought to the total number of years.

2.2.3 Association of coupled ocean-atmosphere phenomena with drought occurrences

The calculations of climate variability indices that related to four major coupled ocean-atmosphere phenomena of influence for the GHA adopted the climatology of 1976-2005 (i.e., 30-year period centered 1990). This is consistent with the current IPCC baseline for climate change assessment.

(1) The ONI is calculated as running 3-month mean SST anomaly for the Niño 3.4 region (i.e., 5^oN-5^oS, 120^o-170^oW) (NCEP, 2017).

(2) The IOD is the difference in SST between two areas (hence a dipole) – a western pole in the Arabian Sea (10^oS-10^oN, 50^o-70^oE) and an eastern pole in the eastern Indian Ocean south of Indonesia (10^oS-22^oN, 90^o-110^oE). The index is discussed in Saji et al. (2005).

(3) The inter-decadal Pacific Oscillation (IPO) is an oceanographic/meteorological phenomenon. The index is based on the difference between the SST averaged over the central equatorial Pacific and the average of the SST in the Northwest and Southwest Pacific (Henley et al., 2015). The regions used to calculate the index are: Region 1 (25°N–45°N, 140°E–145°W); Region 2 (10°S–10°N, 170°E–90°W); and Region 3 **(**50°S–15°S, 150°E–160°W).

(4) The NAO is a large scale seesaw in atmospheric mass between the subtropical high (38.7^oN, 9.1^oW) and the polar low (65.4^oN, 25^oW). The index was defined by Jones *et al*. (1997). The index and its main characteristics are widely discussed in Osborn et al. (1999) and Pozo-V´azquez et al. (2000).

Subsequently, the correlation analysis between individual indices was carried out on grid-cell basis, across the GHA region.

3. Results

3.1 Association of rainfall variability with selected coupled ocean-atmosphere phenomena

The correlation of the probability of drought-year occurrence with individual indices of climate variability drivers are exhibited in **Figure 1** for ONI, IOD, IPO and NAO. The figure shows that the association of drought with the drivers of climate variability is not uniform across the GHA region, and more importantly the association can be of opposite direction. Positive and negative correlations with ONI indicate where El Niño and La Niña induce droughts, respectively. Similarly, the positive and negative correlations with IOD, IPO and NAO indicate when positive and negative modes induce drought conditions, respectively. Given the temporal (i.e. annual) level of association, the magnitudes of the correlation coefficients are arguably not expected to be high, rather, good enough to display the spatial patterns of the association direction.

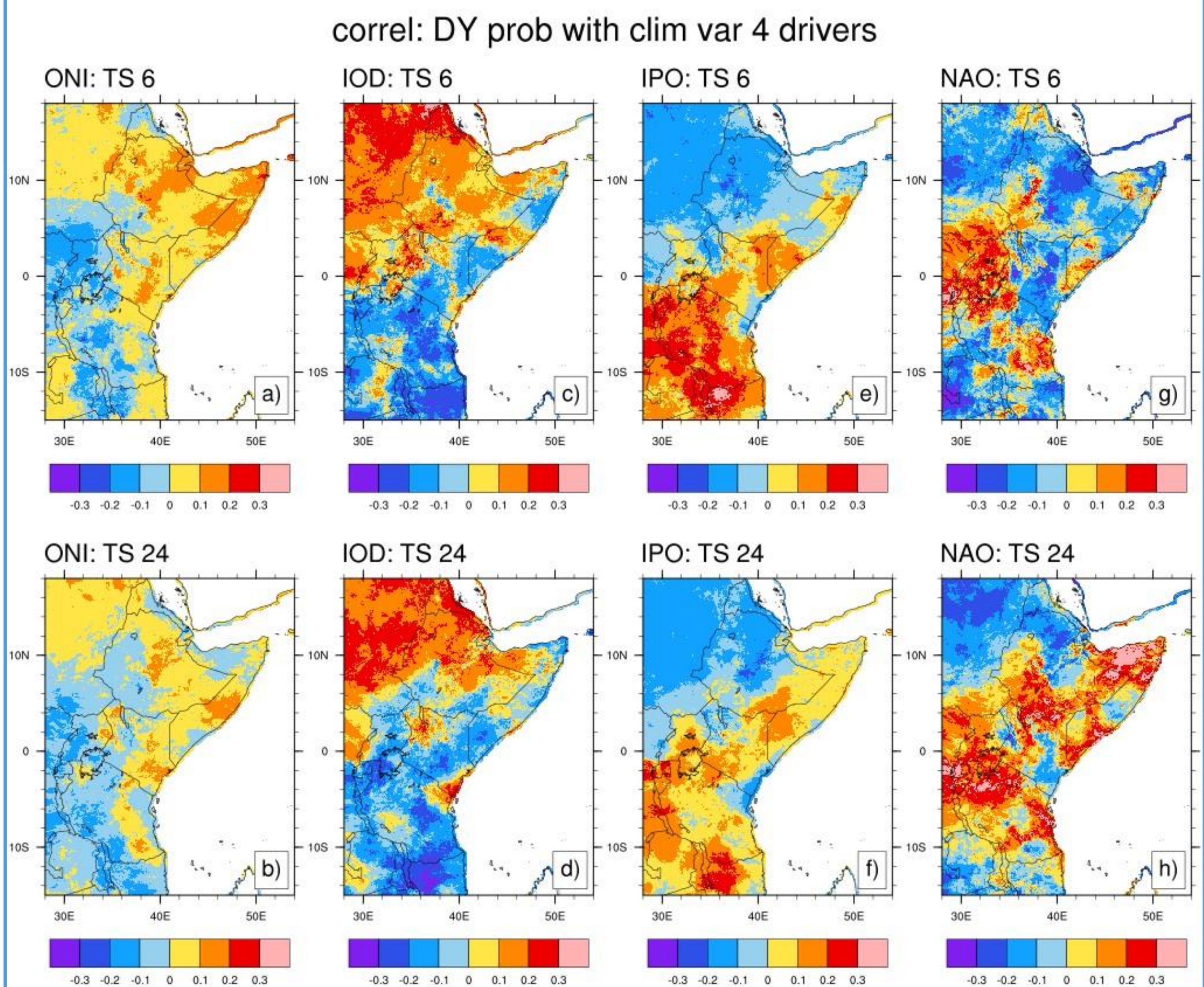

***Figure 1**: Correlation coefficients of drought-year probability with ONI, IOD, IPO and NAO for 6- and 24-month drought timescales: panels [(a), (c), (e), (g)] and [(b), (d), (f), (h)], respectively. Positive and negative correlations with ONI indicate where El Niño and* La Niña *induce droughts, respectively. Similarly, the positive and negative correlations with IOD, IPO and NAO indicate where when they are in positive and negative modes induce drought conditions, respectively. The IOD and IPO for TS6 have exactly opposite spatial patterns regionally (IOD is negatively correlated in the north and positively correlated in the south, whereas the IPO is exact opposite).*

Details of the areal extent of positive and negative associations of drought-year occurrences at 3-, 6-, 12- and 24-month time-scales with individual drivers are given in

Table 1 for the seven GHA Member States. The proportions of the area for each Member State indicate that El Niño driven droughts (positive ONI correlation with) affect 19% of the area of Eritrea, prominently for the 3-month time-scale drought; also19% for Ethiopia (6-month time-scale); 14 – 40% for Somalia, and 7-43% for Kenya across all drought time-scales. On the other hand, the La Niña driven droughts (negative ONI correlation) affect 7-15% of Sudan across the four drought time-scales; 4% and 8% for Kenya, at 3-, and 12-month drought time-scales. The La Niña driven droughts affect Uganda the most (30-60% of the area) across all drought time-scales; followed by Tanzania (about 10-38%).

The area proportion exhibiting IOD positive correlation with drought occurrence is highest for Eritrea, Ethiopia, and Sudan (74-96% across all time-scales). This influence decreases to 14 – 40% over Somalia, 12-29% for Kenya, 6-37% over Uganda and less than 6% for Tanzania. Conversely, the negative IOD correlation is demonstrated over 26% of Somalia, 34% for Kenya, 31% and 64% for Uganda and Tanzania, respectively. The IPO positive correlation with drought occurrences in Somalia, Kenya, Uganda and Tanzania covers up to 85% of the area. On the other hand, IPO is negatively correlated with drought occurrences in Eritrea, Ethiopia and Sudan, over 25-88% of the area across the 4 drought time-scales. The proportion of area coverage of positive NAO for Uganda is 67-90%, Tanzania (30-63%), Kenya (27-90%), Somalia (12-63%), Sudan (13-23%), and only 10% over Ethiopia for 24-month timescale. On the other hand, the negative NAO correlation covers 26-46% of Eritrea, Sudan (10-30%), Somalia (25-35%), and 11-24% for Kenya, Uganda and Tanzania.

Table 1: *Areal extent (%) of regions where drought years at 3-, 6-, 12- and 24-month time-scales are positively or negatively correlated (coefficient magnitude greater than 0.1) with individual drivers of rainfall variability, namely the Oceanic Niño* Index *(ONI), Indian Ocean Dipole (IOD), Inter-decadal Pacific Oscillation (IPO) and Northern Atlantic Oscillation (NAO).*

Region	Drought time-scale	Proportion (%) under positive correlation				Proportion (%) under negative correlation			
		ONI	IOD	IPO	NAO	ONI	IOD	IPO	NAO
Eritrea	3	18.92	72.34	0.00	5.69	0.54	0.29	24.70	41.06
	6	8.98	94.39	0.00	6.45	2.14	0.00	45.55	26.31
	12	4.56	86.04	0.00	0.66	0.47	0.00	46.01	46.01
	24	2.46	96.39	0.00	1.31	2.91	0.00	60.71	42.06
Ethiopia	3	8.30	91.86	0.27	2.82	0.11	0.27	87.43	11.10
	6	18.82	82.46	0.51	2.12	0.09	0.39	86.79	7.75
	12	3.74	88.49	0.69	7.56	0.86	0.69	86.90	7.22
	24	2.05	87.43	2.08	10.45	0.11	1.62	33.78	6.34
Sudan	3	1.47	75.14	7.95	13.81	12.21	9.57	62.64	24.31
	6	0.62	89.02	0.00	21.69	14.74	0.00	79.21	30.18
	12	0.00	74.39	0.00	23.28	12.07	0.43	68.96	10.51
	24	0.00	72.58	0.00	15.75	7.32	3.30	67.04	20.72
Somalia	3	27.57	39.93	25.53	11.72	0.00	26.30	3.54	24.66
	6	40.42	24.00	25.98	12.51	0.02	25.68	3.58	34.58
	12	21.51	14.04	19.85	22.14	0.78	22.99	1.69	13.12
	24	14.35	15.63	16.40	62.54	0.10	27.56	0.12	1.93
Kenya	3	43.15	13.77	27.53	12.74	4.24	65.46	2.66	61.66
	6	15.26	12.28	26.00	7.83	1.35	23.92	17.83	41.36
	12	6.68	13.67	15.63	68.69	7.56	19.71	5.95	14.83
	24	20.24	29.42	16.07	27.64	1.19	25.48	38.33	11.35
Uganda	3	0.31	13.13	31.93	67.61	31.39	43.41	1.02	5.04
	6	0.03	37.20	13.31	89.69	60.72	2.37	7.13	0.03
	12	0.00	3.60	29.83	77.79	31.24	36.31	3.90	0.00
	24	3.84	5.87	30.87	66.99	29.63	41.46	1.74	3.65
Tanzania	3	1.34	5.74	72.72	63.49	37.24	52.72	0.62	11.00
	6	0.17	2.45	84.57	37.87	16.98	66.14	0.74	22.13
	12	0.26	3.85	74.74	30.43	8.96	75.84	2.94	24.36
	24	2.70	2.66	34.27	62.96	15.36	63.26	1.94	1.82

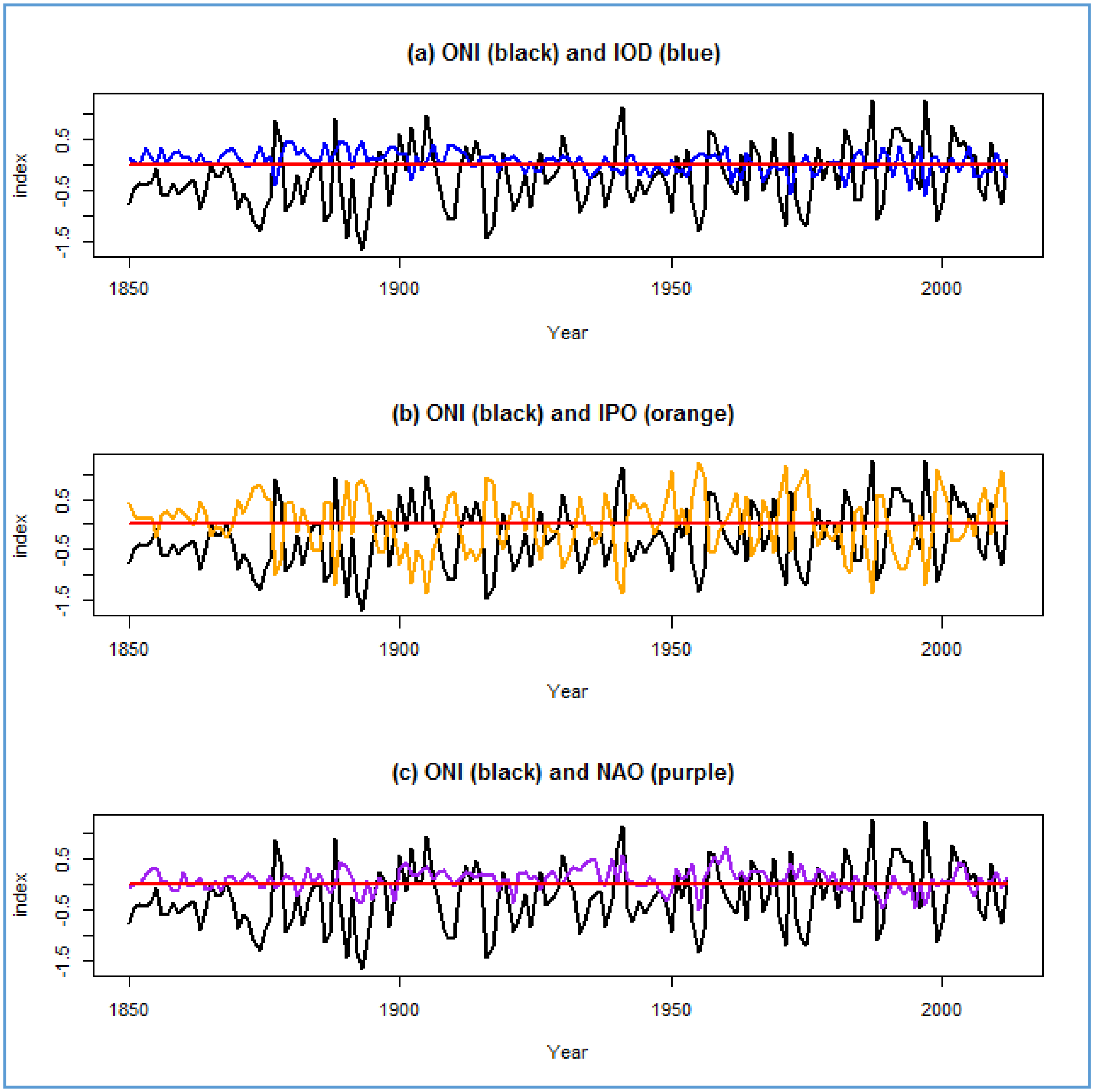

Figure 2: *Comparison of variability of annual mean of ONI with (a) IOD, (b) IPO and (c) NAO for the period 1850 to 2012. Complex interactions manifest between modes of these 4 major climate variability drivers. For example, ENSO extends its influence on modes of IOD and NAO, which in turn feed back onto ENSO (Kajtar et al., 2017). The interactions between pairs of modes can alter their strength, periodicity, seasonality, and ultimately their predictability.*

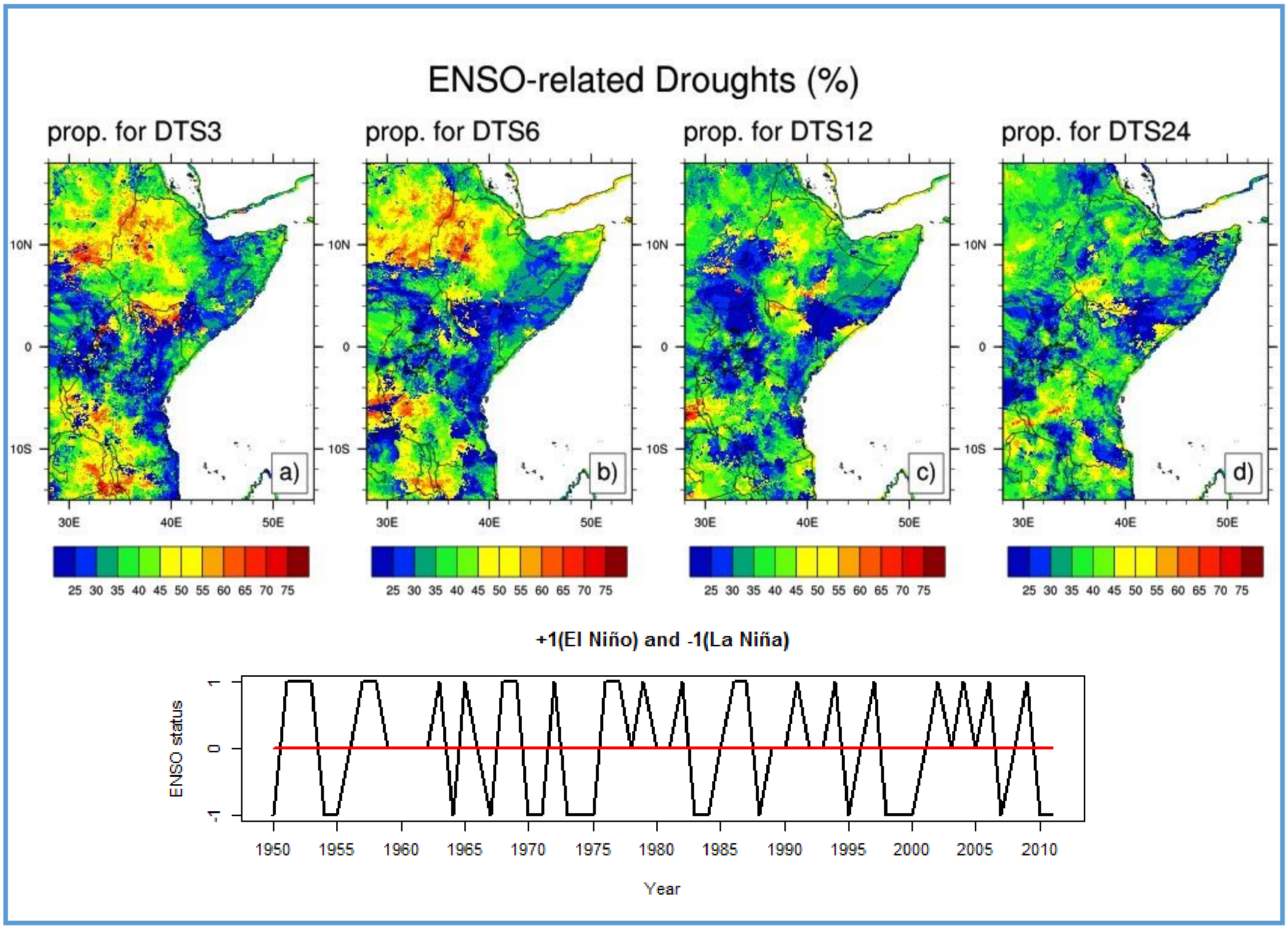

Figure 3: *Proportion (%) of ENSO-related drought-year occurrences to the total drought-year occurrences for the 1950-2012 period. It is evident in the observations that not all droughts are ENSO driven. The highest proportions of about 70% of drought-year occurrences are demonstrated at 3- and 6-month and generally much lower proportions (< 30%) at 12- and 24-month timescales, respectively.*

3.2 Reliability of ENSO in drought prediction

Almost all drought studies reiterate the influence of ENSO phenomenon on drought occurrences, with respect to drought prediction. However, surprisingly, many of them do not go beyond correlation analysis (Hafez, 2016, Beltrando and Camberlin, 1993), that merely suggests the potential teleconnection without desired explicit relationships. The main challenge is to account for the interactions of different systems of climate variability and their teleconnections. The overall influence of climate variability drivers depends on their concurrent modes (Behera et al., 2006). Therefore, this is the main source of uncertainty in the prediction of climatic extremes including droughts when the prediction is solely based on ENSO phenomenon (Kane, 1997).

Although ENSO is generally acknowledged to play a major role in triggering worldwide extreme climatic events, it is evident in the observations and models that not all droughts are ENSO driven (Cai, 2015). This is demonstrated in **Figure 3** where proportions of drought-year occurrences in ENSO years to the total number of drought-year occurrences over the GHA region are shown for the 1950-2011 period. Here, an ENSO year refers to a year in which ENSO is either in El Niño or La Niña mode, as distinguished from a normal/neutral year (BoM, 2017). Generally, ENSO-driven droughts are dominant over Sudan, Eritrea, most of Ethiopia except the south-eastern areas, Somalia, western and south-western Tanzania. However, the highest proportions of about 70% of drought-year occurrences are demonstrated at 3- and 6-month timescales (DTS3 and DTS6, respectively) and generally much lower proportions (< 30%) at 12- and 24-month timescales (DTS12 and DTS24, respectively).

3.3 Drought characteristics

Drought characteristics derived here include drought frequency (in terms of probability of drought-year), duration, and areal-extent of drought events. The importance of these elements are based on the view that duration (persistence) is a major determinant factor of drought severity (i.e., extent of impact devastation), in that once drought is declared, the impacted system gets incapacitated. Therefore, severity becomes a function of drought duration and at state or institutional level, the drought areal-extent exacerbates the challenge in terms of mitigation.

3.3.1 Probability of drought-year occurrences

Long-term probability of drought-year occurrences across the GHA region range from 20 to 30%, except for isolated areas which show probabilities of 10-20% and 30-40% on the low and high sides, respectively. The probabilities of drought-year occurrences are similar for all drought time-scales for most of the areas as shown in **Figure 4** for the 6- and 24-month drought timescales in panels (a) and (e), respectively. However, patches of relatively higher probabilities become more pronounced for the 3- and 12-month (not shown) time-scales. Generally, there is consistency in drought-year occurrences, as indicated by the small range of probability variance (**Figure 4**, panels (b) and (f)).

Nevertheless, the long-term trends in the probability of drought-year occurrences (**Figure 4**, panels (c) and (g) in conjunction with (d) and (h), respectively, suggest a general increase of the probability of drought-year occurrences in the north-eastern and some parts to the south of the region. For the drought-year at short timescale, significant increase is evident over north-eastern Ethiopia, Somalia, Kenya and some parts of Tanzania. The increases become more pronounced for droughts at the 3- and 12-month (not shown) timescales, with increases in the probability of occurrences of up to +0.4% per decade. Elsewhere, there is a general tendency of decrease in the probability of drought-year occurrences up to -0.2% per decade on the average. However, the decreases are not as significant as for the increase trends where applicable.

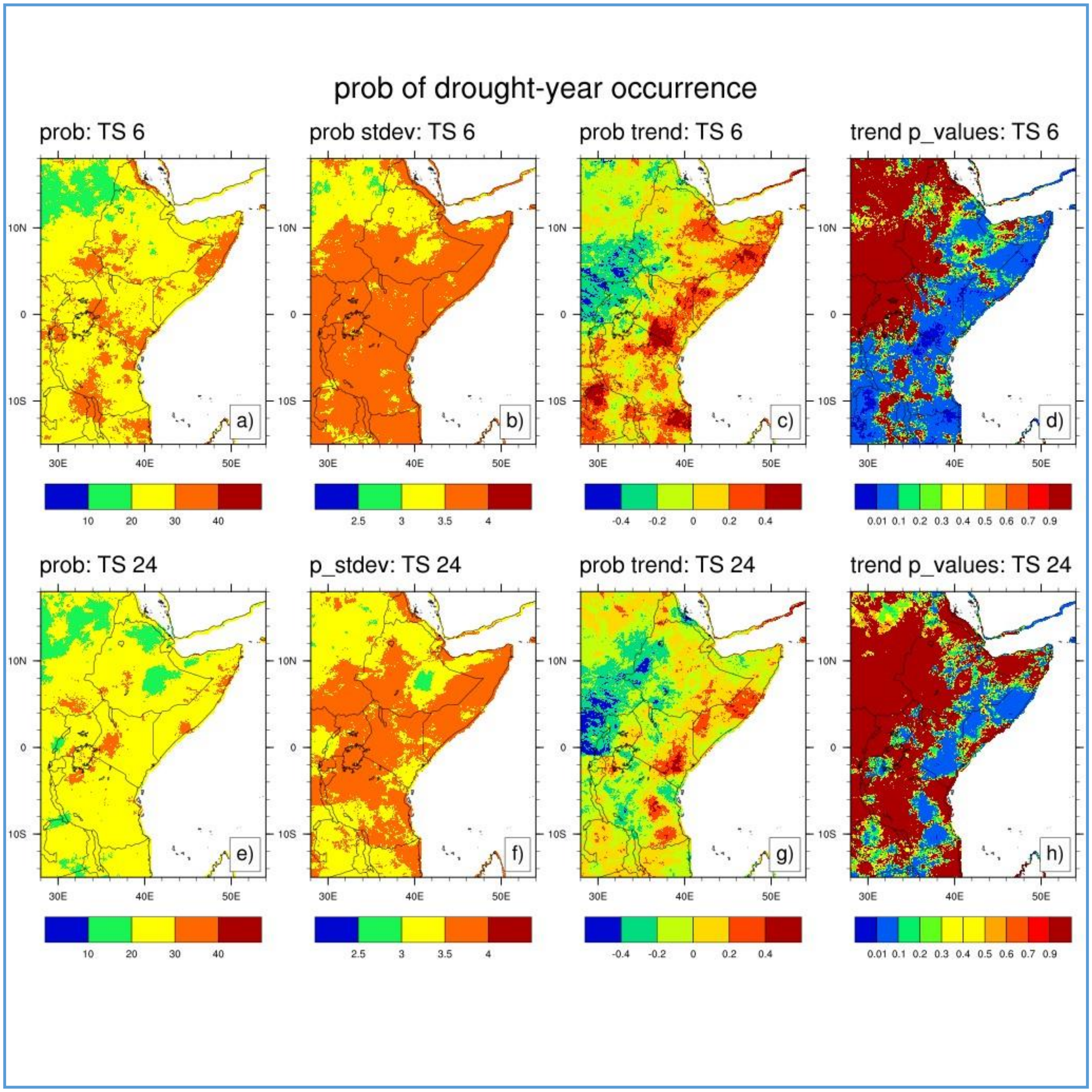

Figure 4: *Long-term drought-year probability (%), standard deviation (%), trend (% per decade) and their p_values for 6- and 24-month drought time scales: panels (a) through (d) and (e) through (h), respectively. It is evident that the long-term probability of drought-year occurrences across the GHA region range from 20 to 30%, except for isolated areas, which exhibit probabilities as low as 10% and up to 40% on the lower*

and higher cases, respectively. This reaffirms drought to be an intrinsic part of the GHA landscape.

3.3.2 Duration of drought events

Drought events exhibit drought duration of about 4, 5-7, 6-14 and 8-24 months for the 3-, 6-, 12- and 24-month timescales, respectively for half of the time as shown by the 50th percentiles. On the other hand, the 90th percentile durations suggest that 1 out of 10 droughts at short timescales can persist for 3 – 18 months. At higher (12- and 24-month) timescales, drought persistence exhibit longer duration of up to 36 and 72 months, respectively. **Figure 5** demonstrates the 50th and 90th percentiles of drought durations for 6- and 24-month timescales in panels (a) and (b); and (e) and (f), respectively.

The results show a tendency of decreasing trend in drought duration of up to 2 months/decade over most of Uganda and central Tanzania (extending to the north-eastern and south-western areas) for droughts at 3- and 6-month timescales. For droughts at 12-month timescales, the decreasing trend becomes widespread over Tanzania, eastern Kenya, southern and northern Somalia and south-western Ethiopia. For most of the northern sector of the GHA (Sudan, Eritrea, Ethiopia, Somalia and northern Kenya) an increasing trend in drought duration is evident for the 3- and 6-month timescales. On the contrary, for the droughts at 24-month timescale, the entire region exhibits steep positive trends in drought duration (up to a few years per decade), except over the south-western Tanzania. This pattern is demonstrated in **Figure 5** panels (c) and (g) for the 6- and 24-month timescales.

However, the respective p-values from a statistical test of non-zero trend significance (α=0.05) shown in panels (d) and (h), suggest that these trends in duration of drought events are not statistically significant. This is consistent with results of other studies worldwide (McCabe and Wolock, 2015, Awange et al., 2016), also as reported in the more recent IPCC special report (SREX), that there is no clear evidence of trends in the observed drought characteristics (IPCC, 2012).

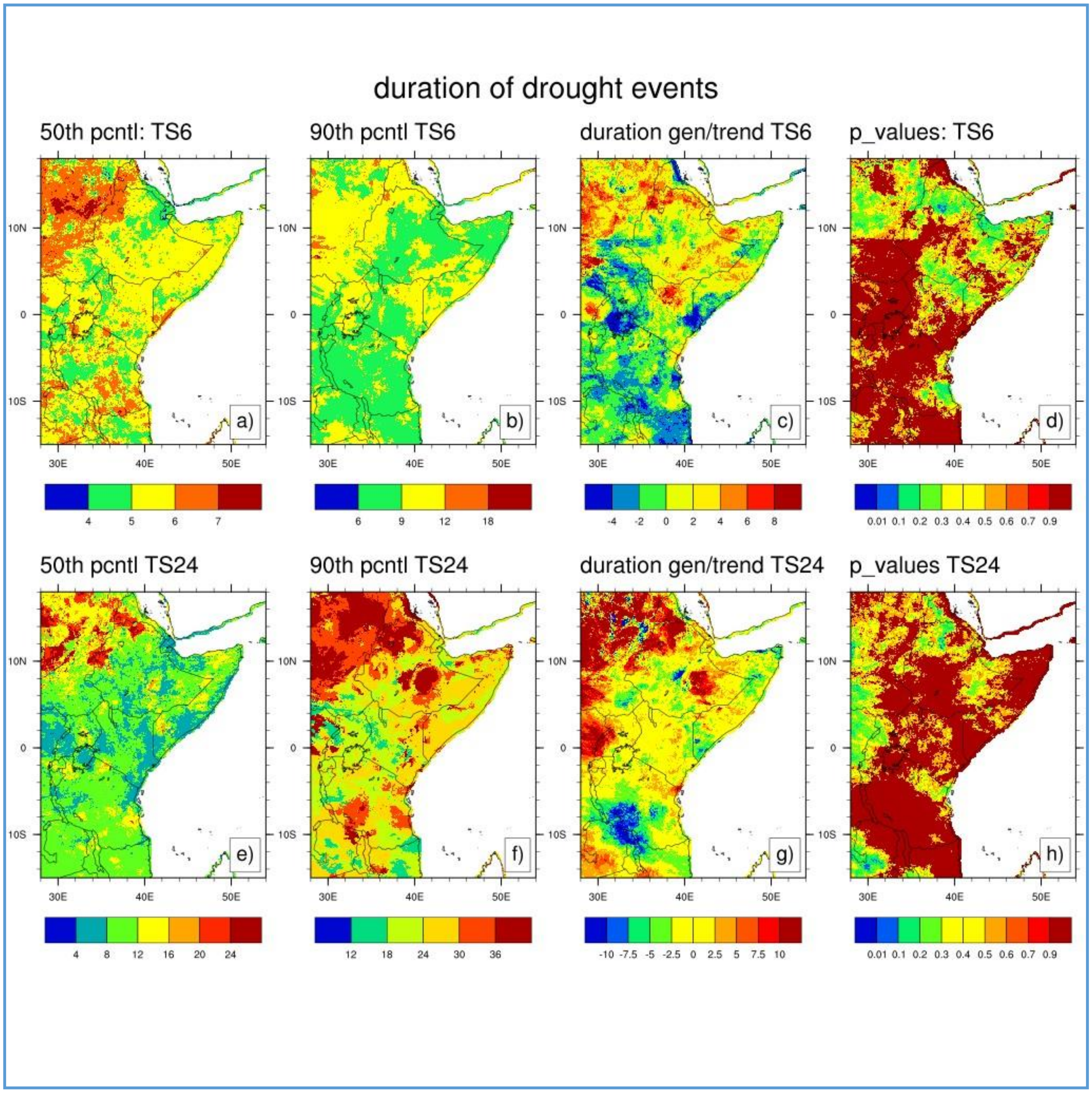

***Figure 5**: The 50^{th} and 90^{th} percentiles of drought durations for 6- and 24-month timescales in panels (a) and (b); and (e) and (f), respectively. Long-term trend in general duration (months/decade) of droughts at 6- and 24-month time-scales in panels (c) and (g), with their respective p-values from a statistical test of non-zero trend significance at 0.05 alpha (panels (d) and (h). The duration of more than half of the drought events is up to 7 and 24 months for the 6- and 24-month timescales, respectively. On the other hand, the 1 out of 10 drought events, can persist for up to 18 months (6-month timescales). Droughts at 24-month timescale, tend to persist much longer (>= 36 months). Nevertheless, there is no significant trend in drought duration.*

3.3.3 Drought areal-extent

Another important element for drought risk assessment is the areal-extent (% of total land area) experiencing drought at a time. **Figures 6 and 7**, show that there is remarkable variability in drought areal-extent over years. For example, around the period 1910-1925, the GHA region, experienced droughts covering up to 80% of the area, and only about 20% for the 1930-1960. Then after the 1960s, drought areal-extent is shown to be on the rise, even beyond the 1910-1925 levels in the last decades. However, there is a general increasing trend representing an overall increase of 22% in the region over the course of the 20th Century and the first decade of the 21st Century. For some of the individual Member States, the proportion almost doubled, while others shrunk considerably, as detailed below.

However, due to the differences in responses to drought drivers across the region, (discussed in Section 3.1), the drought areal-extents among Member States of the GHA region also differ. Increasing trends of 0.26-0.34% per annum over Sudan; +0.10% for Eritrea; +(0.34-0.40)% over Ethiopia; +(0.13-0.35)% for Somalia; +(0.04-0.10)% over Kenya; -0.10 to +0.04% for Uganda; and -0.13 to +0.01% over Tanzania are demonstrated. In the aspect of drought areal-extent, therefore, the threat is real for the GHA region in general, except for Tanzania and Uganda to a lesser extent where decreasing trends are evident for drought timescales greater than six months.

Increasing trends in drought areal-extent have serious implications that include worsening food security and water availability, straining the resilience of communities across the region. In Somalia alone, the number of people needing assistance has risen from five million in September 2015 to over 6.2 million in February 2017 (more than half the country's population). This includes a drastic increase in those facing "crisis" and "emergency" situations, from 1.1 million six months ago to a projected 3 million between February and June 2017 (UNISDR, 2017). Similar situation can be said for South Sudan, Ethiopia, and some parts of Kenya. For example, Ethiopia has appealed for US$948 million to address emergency needs for 5.6 million people for 2017. This is almost a 50-percent reduction in the number of food insecure people, which reached 10.2 million in 2016, as reported by the UNISDR (2017).

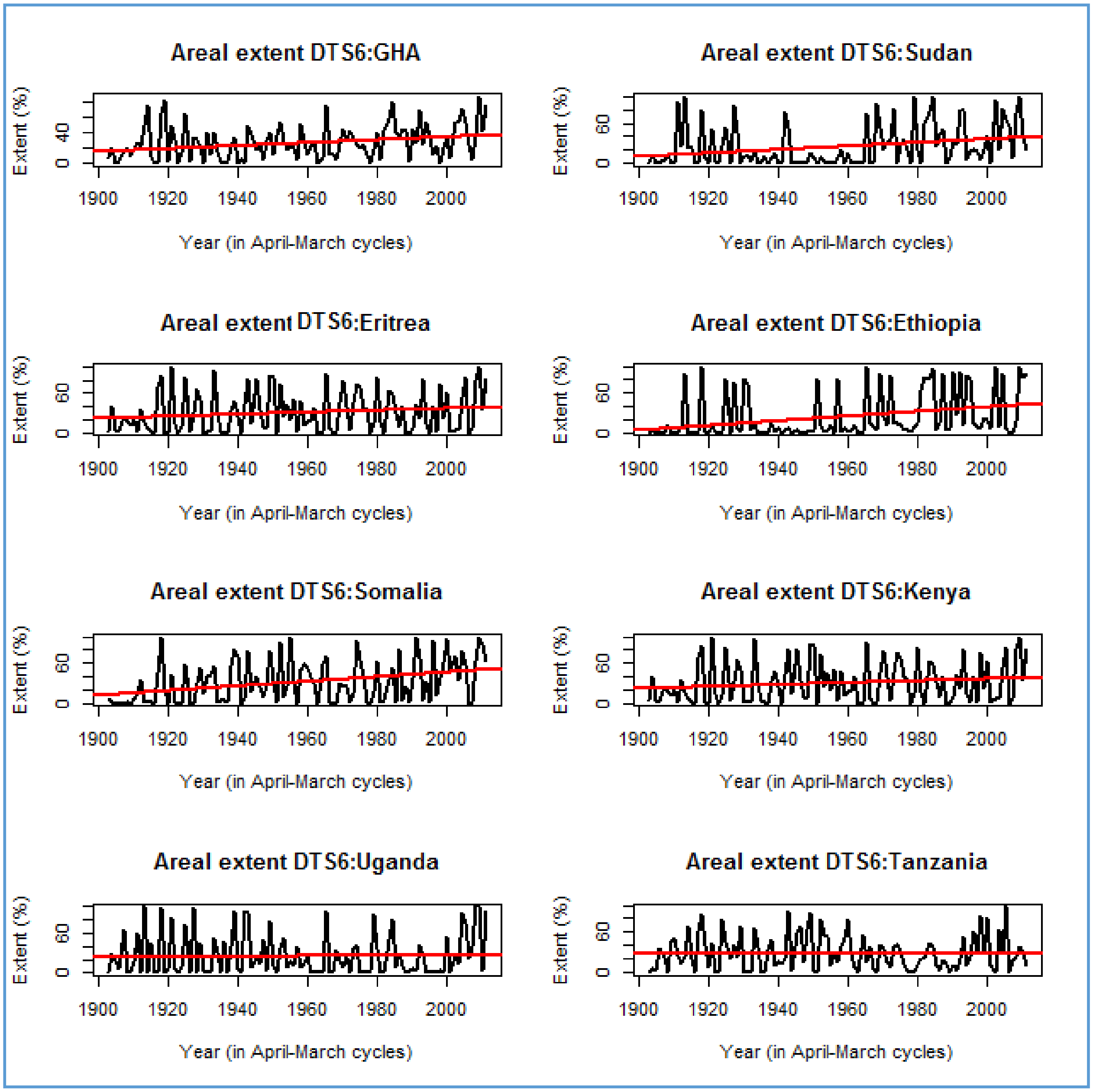

Figure 6: *Areal-extent (% of total land area) (black) and a trend line (red) of +0.20, +0.28, +0.10, +0.36, +0.35, +0.15, +0.04 and -0.01 (percent/annum) over the GHA region Members States: Sudan, Eritrea, Ethiopia, Somalia, Kenya, Uganda and Tanzania, respectively, for the 6-month timescale droughts of 1903-2012 annual (April-March) cycles.*

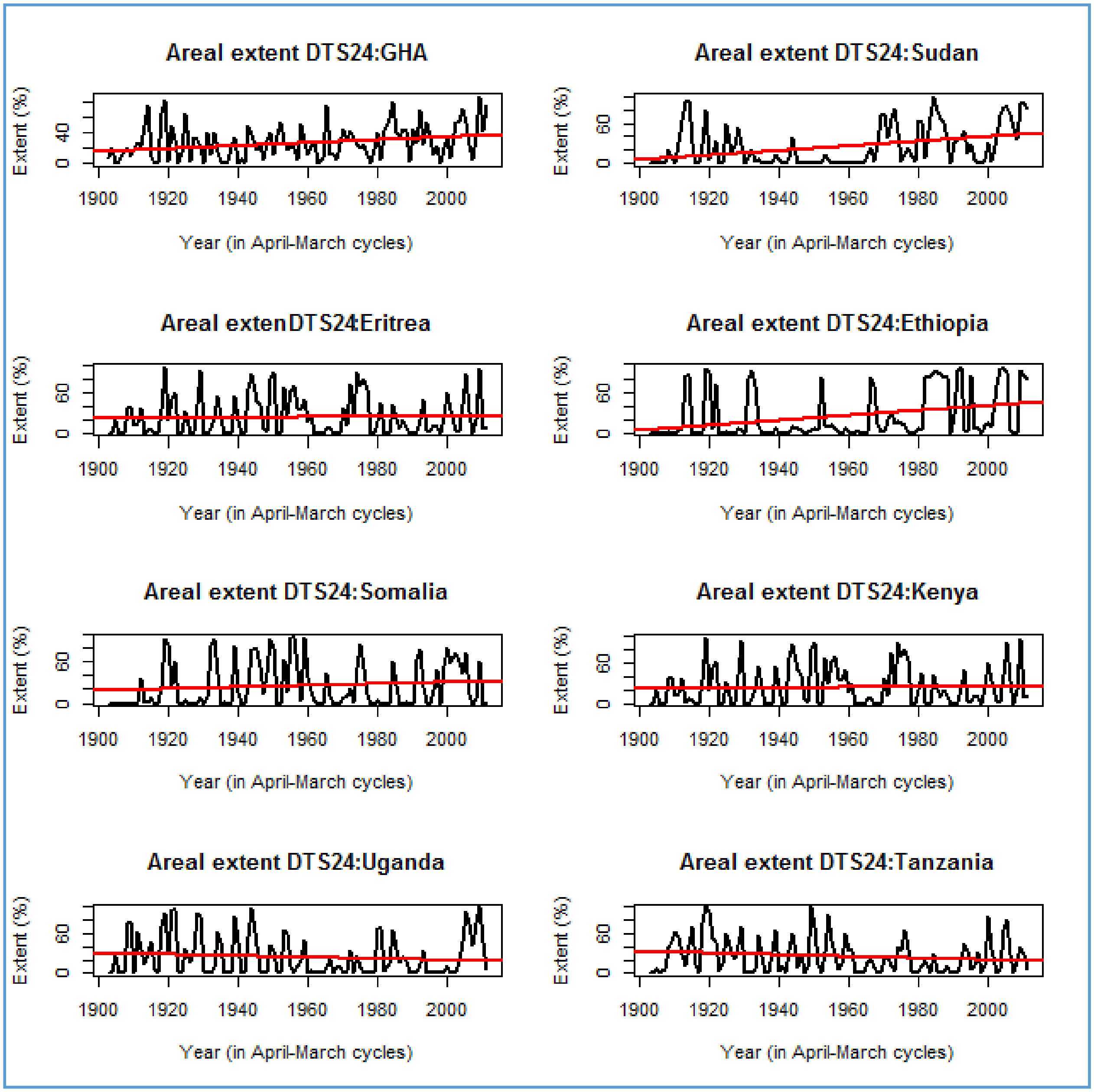

Figure 7: *Areal-extent (% of total land area) (black) and trend line (red) of +0.20, +0.34, +0.10, +0.35, +0.13, +0.04, -0.10 and -0.13 (percent/annum) over the GHA region Member States, Sudan, Eritrea, Ethiopia, Somalia, Kenya, Uganda and Tanzania, respectively, for the 24-month timescale droughts of 1903-2012 annual (April-March) cycles.*

3.5 Trends in rainfall

The spatial distribution of mean annual rainfall and its trend in ***Figure 8***, panels (a) and (b), respectively, show that relatively wet regions such as the Lake Victoria basin are getting wetter and dry regions like Somalia and northeastern Ethiopia are getting drier. This process is often referred to as “amplification of the water cycle”, associated with global warming in previous studies. Earlier studies indicated that the amplification of the water cycle was happening at 7% per 1°C of global warming (Huntington, 2006). However, a new study (Skliris et al., 2016) suggests that the amplification is happening at about 3 – 4% per 1°C. This is probably due to a weakening of the atmospheric circulation which transports freshwater from the dry to wet regions of the globe.

Nevertheless, the low level of statistically significant rainfall trends demonstrated over the GHA from our study, particularly the drying trend, also suggests a slower amplification process than first thought. The agreement between recent results from climate models (Skliris et al. 2016) and observations (analyzed here) over the recent past is another important finding of this study because it adds confidence to climate model projections of water cycle amplification under greenhouse gas emission scenarios.

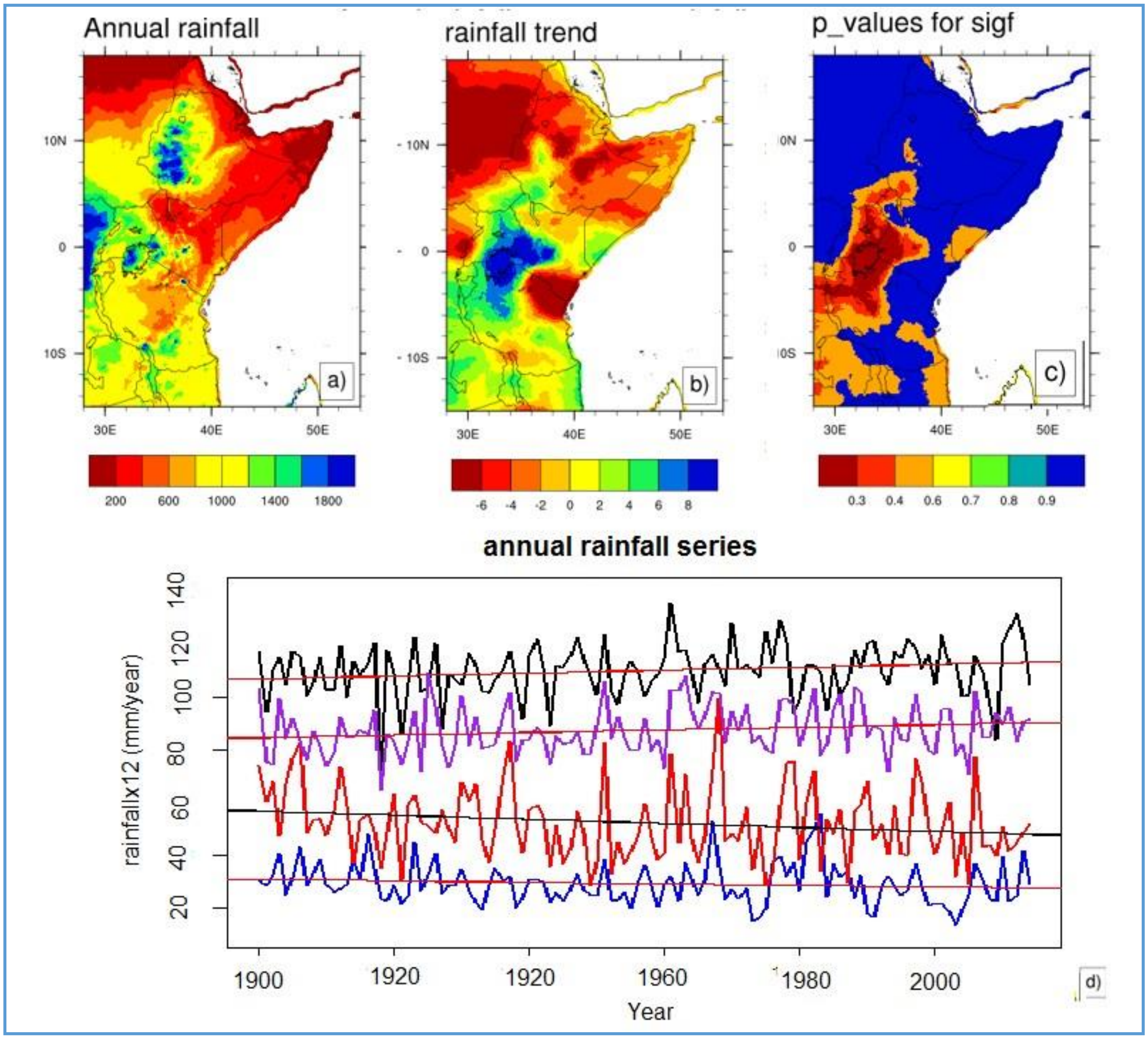

Figure 8: *Spatial distribution of annual (a) mean rainfall (mm/year); (b) rainfall trend (mm/decade); (c) p_values for trend statistical significance; and (d) rainfall time series (1900-2014) for selected grid-cells: Uganda (2.4^{o}N, 33.2^{o}E) black; Tanzania (4.3^{o}N, 30.7^{o}E) purple; Kenya (-2.7^{o}N, 38.3^{o}E) red; and Ethiopia (7.6^{o}N, 42.5^{o}E) blue. Panels (a) and (b) portray a tendency of relatively dry areas becoming drier and relatively wet areas getting wetter. However, panel (c) shows only a low level of statistical significance in these trends.*

4. Discussion

The results show remarkable spatial variations in the association of the probability of drought occurrences with ENSO, IOD, IPO and NAO. These climate variability drivers tend to either enhance or suppress or displace the time/region dependent effect of weather systems (Riddle and Cook, 2008). The abnormities imposed on the effects of weather systems that include (1) the inter-tropical convergence zone (ITCZ), (2) monsoon/trade winds, (3) ridges, and (4) jet systems, are dependent on the status of modes of the prevailing drivers at a time.

Naturally, complex interactions manifest between modes of these four major climate variability drivers. For example, ENSO extends its influence on modes of IOD and NAO, which in turn feed back onto ENSO (Kajtar et al., 2017). The interactions between pairs of modes (**Figure 2**) can alter their strength, periodicity, seasonality, and ultimately their predictability. It is thought that the IOD has a link with ENSO events through an extension of the Walker Circulation to the west and associated Indonesian flow of warm tropical ocean water from the Pacific into the Indian Ocean (Kajtar et al., 2017). Hence, positive IOD events are often associated with El Niño and negative events with La Niña. When the IOD and ENSO are in phase, the impacts of El Niño and La Niña events are often most extreme, while when they are out of phase the impacts of El Niño and La Niña events can be diminished. For example, the observed relatively bigger (areal-extent) influence of IOD on droughts than anomalies associated with the ONI, particularly over Eritrea, Ethiopia, Somalia and Kenya (Table 1) can be explained as a result of the thermodynamics in the mid-troposphere related to the extension of the tropical warm pool westwards (Williams and Funk, 2011).

Kajtar et al. (2017) found that IOD variability has a net damping effect on ENSO and NAO variability, and conversely each promote IOD variability. They also demonstrated a weak damping influence by NAO on ENSO, and an enhancing influence by ENSO on NAO variability. The potential interactions between the NAO and ENSO in influencing regional latitudinal inter-tropical convergence zone (ITCZ) shifts are discussed in McHugh and Rogers (2001). They evaluated moisture and circulation field variations associated with NAO and showed that precipitable water over the region varies significantly such that anomalously high (low) convective rainfall occurs to the southern areas when the NAO is weak (strong).

On the other front, the IPO fluctuations are less understood due to being less frequent than other climate variability drivers. However, notably during the 20th century, there were negative IPO phases in 1925-1946 and 1978-1998 (**Figure 2b**); and a positive phase from 1947 to1976. Of interest is the fact that El Niño events increased between 1978 and 1998, therefore it is reasonable to speculate that IPO may be linked to ENSO events and to SST changes in general. In other words, SST changes may cause the IPO and not the other way round (Salinger et al., 2001). However, given its long cycle periods, it will be some time before IPO is understood to the same level of detail as other indices.

While ENSO is often solely considered in drought prediction, our results demonstrated that not all droughts are ENSO driven. For the GHA, ENSO-driven droughts were found dominant only over Sudan, Eritrea, most of Ethiopia except the south-eastern areas, Somalia, western and south-western Tanzania. However, the highest proportion of ENSO-driven drought-year occurrences is about 70% for the 3- and 6-month timescales, otherwise generally much lower proportions (< 30%) for the 12- and 24-month timescale droughts.

The spatial distribution of drought-risk parameters and the patterns of drought occurrence association with climate variability drivers revealed complex zonality. For example, over the northern and north-eastern areas drought occurrences are associated with El Niño, positive mode IOD, negative modes of IPO and NAO (with well-defined patterns at short timescales). The converse holds for the southern and south-western areas (e.g., occurrences of droughts are associated with La Niña). While the range of long-term probabilities of drought-year occurrences across the GHA region is understandably small (20-30%), the northeastern areas experience more persistent droughts than elsewhere. Similarly, the tendency of increases in drought areal-extent is more pronounced to the northern and north-eastern sectors of the region.

In addition, the trends in annual rainfall show that relatively wet regions (e.g. the Lake Victoria basin) are getting wetter while the converse is true for dry regions (e.g. Somalia and northeastern Ethiopia). However, these trends are of low statistical significance over the study period. This is consistent with findings of Skliris et al. (2016), suggesting a slower water cycle amplification process associated with climate change than first thought. The agreement between climate models and observations over the recent past is another important finding as it adds confidence to climate model projections. However, in the context of drought occurrences, this systematic rainfall reduction does not necessarily translate into drought events. Arguably, it could simply mean a change in rainfall regime towards new aridity levels. Thus, the management strategies could be different from those relevant to drought events.

5. Conclusions

This study sought to quantify the variation of influence among climate variability drivers across the region; establish drought characteristics that underpin drought impacts management; and examine consistency of increase in drought-like crises with trends in drought characteristics over the GHA region. The study concludes that:

1. El Niño driven droughts affected 19% of the area for Eritrea and Ethiopia at 3- and 6-month timescales, respectively; 14 – 40% for Somalia; and 7-43% for Kenya across all drought timescales while the La Niña driven droughts affected 7-15% of Sudan, across the 4 drought time-scales; 4% and 8% for Kenya, at 3-, and 12-month drought timescales, respectively. The La Niña driven droughts affect Uganda most, affecting 30-60% of the area across all drought time-scales; and about 10-38% for Tanzania. Similarly, there is substantial variations in area proportions affected by IOD, IPO and NAO phenomena.

2. The long-term probability of drought-year occurrences across the GHA region range from 20 to 30%, except for isolated areas, which exhibit probabilities as low as 10% and up to 40% on the lower and higher cases, respectively. There is no statistically significant trend in the probability of drought-year occurrences.

3. The duration of more than half of the drought events is up to 4, 7, 14 and 24 months for the 3-, 6-, 12- and 24-month timescales, respectively. On the other hand, the 1 out of 10 drought events, can persist for up to 18 months (the 3- and 6-month timescales). Droughts at the 12- and 24-month timescales tend to persist much longer (≥ 36 months). However, there is no significant trend in drought duration. By contrast, the drought areal-extent has shown generally increasing trends. On the average (across drought timescales), trends per decade of 3%, 1%, 3.7%, 2.4%, 0.7%, -0.3% and -0.6% were found for Sudan, Eritrea, Ethiopia, Somalia, Kenya, Uganda and Tanzania, respectively.

4. The results also show weak trends for the relatively wet areas (e.g. the Lake Victoria basin) getting wetter while the dry areas (e.g., Somalia and northeastern Ethiopia) becoming drier. These weak trends are consistent with Skliris et al. (2016) findings and indicate a slower water cycle amplification process than first thought. The agreement between climate models and observations over the recent past is an important finding, as it adds confidence to climate model projections.

5. In addition, since there is no evidence of substantially significant changes in drought characteristics, the peculiarity of drought-like crises in the GHA can be attributed to unaccounted for systematic rainfall reduction (among other factors reported elsewhere). This highlights the importance of distinguishing drought impacts from those associated with new levels of aridity. In principle drought is a temporary phenomenon while aridity is permanent, require deferent management strategies.

Acknowledgements

The authors would like to acknowledge scientists from the UC Santa Barbara Climate Hazards Group and Florida State University for the Centennial Trends and the Climatic Prediction Centre- NOAA for the SST data.

References

AWANGE, J., MPELASOKA, F. & GONCALVES, R. 2016. When every drop counts: Analysis of Droughts in Brazil for the 1901-2013 period. *Science of the Total Environment* 566-567, 1472-1488.

BAROODY, J. 1995. *Anatomy of an Overthrow: Why a Revered African Leader was Toppled.* *http://adst.org/2016/10/anatomy-overthrow-revered-african-leader-toppled/* [Online]. Association for Diplomatic Studies and Training. [Accessed 6th February 2017].

BEHERA, S. K., LUO, J., MASSON, S., RAO, S. A., SAKUMA, H. & YAMAGATA, T. 2006. A CGCM study on the interaction between IOD and ENSO. *Journal of Climate,* 19**,** 1688-1705.

BELTRANDO, G. & CAMBERLIN, P. 1993. Interannual variability of rainfall in eastern horn of Africa and indicators of atmospheric circulation. *International Journal of Climatology,* 13**,** 533-546.

BOM. 2017. *The three phases of the El Niño–Southern Oscillation (ENSO): http://www.bom.gov.au/climate/enso/history/ln-2010-12/three-phases-of-ENSO.shtml* [Online]. Beurau of Meteorology, Australia. [Accessed 12 April 2017].

CAI, W. 2015. *What is El Nino and why does it have so much influence over our weather?: http://www.abc.net.au/news/science/2015-12-09/el-nino-what-is-it-and-why-does-it-matter/6908126* [Online]. ABC Science. [Accessed 8 March 2017].

COOK, E. R., J. E., COLE, R. D., D'ARRIGO, D. W. S. & VILLALBA, R. (eds.) 1999 *Tree ring records of past ENSO variability and forcing* Cambridge, U.K.: Cambridge Univ. Press.

CORDERY, I. & MCCALL, M. 2000. A model for forecasting drought from teleconnections. *Water Resources Research,* 36**,** 763-768.

EVANS, M., HASTINGS, N. & PEACOCK, B. 2000. Statistical Distributions. *Beta Distribution.* 3 ed. New York: Wiley.

FAO 2007. Evaluation of the FAO Emergency and Rehabilitation Assistance in the Greater Horn of Africa (2004-2007), Final Report. FAO.

FAO. 2017. *Millions of people face food shortages in the Horn of Africa: http://www.fao.org/news/story/en/item/468941/icode/* [Online]. [Accessed 25 April 2017].

FUNK, C., NICHOLSON, S. E., LANDSFELD, M., KLOTTER, D., PETERSON, P. & HARRISON, L. 2015. The Centennial Trends Greater Horn of Africa precipitation dataset *SCIENTIFIC DATA 2:150050 | DOI: 10.1038/sdata.2015.50*.

GUPTA, A. K. & NADARAJAH, S. (eds.) 2004. *Handbook of Beta Distribution and Its Applications (Statistics: A Series of Textbooks and Monographs) 1st Edition*: CRC Press.

HAFEZ, Y. 2016. Study on the Relationship between the Oceanic Nino Index and Surface Air Temperature and Precipitation Rate over the Kingdom of Saudi Arabia *Journal of Geoscience and Environment Protection,* 4**,** 146-162.

HENLEY, B. J., GERGIS, J., KAROLY, D. J., POWER, S. B., KENNEDY, J. & FOLLAND, C. K. 2015. A Tripole Index for the Interdecadal Pacific Oscillation. *Climate Dynamics,* 45**,** 3077-3090.

HUNTINGTON, T. G. 2006. Evidence for intensification of the global water cycle: Review and synthesis. *Journal of Hydrology,* 319**,** 83–95.

IGAD. 2017. *http://reliefweb.int/report/somalia/statement-igad-executive-secretary-current-drought-greater-horn-africa* [Online]. [Accessed 06 March 2017].

IPCC 2012. Special Report on Managing the Risks of Extreme Events and Disasters to Advance Climate Change Adaptation (SREX). *In:* II, I. W. G. (ed.). Stanford, CA 94305, USA.

JANSSON, K., HARRIS, M. & PENROSE, A. 1987. *The Ethiopian Famine,* London Zed Press.

JOHNSON, N. L., KOTZ, S. & BALAKRISHNAN, N. 1995. *Continuous Univariate Distributions. Voolume 2, 2rd ed. Wiley*

JONES, P. D., JONSSON, T. & WHEELER, D. 1997. Extension to the North Atlantic oscillation using instrumental pressure observations from Gibraltar and south-west Iceland. *International Journal of Climatology* 17**,** 1433-1450.

KAJTAR, J. B., SANTOSO, A., ENGLAND, M. H. & CAI, W. 2017. Tropical climate variability: interactions across the Pacific, Indian, and Atlantic Oceans. *Climate Dynamics,* 48**,** 2173-2190.

KALNAY, E., KANAMITSU, M., KISTLER, R., COLLINS, W., DEAVEN, D., GONDIN, L., IREDELL, M., SAHA, S., WHILTE, G., WOOLLEN, J., ZHU, Y., CHELLIAH, M., EBISUZAKI, W., HIGGINS, W., JANOWIAK, J., MO, K. C., ROPELEWSKI, C., WANG, J., LEETMAA, A., REYNOLDS, R., JENNE, R. & JOSEPH, D. 1996. The NCEP/NCAR 40-year reanalysis project. *Bull. Amer. Meteor. Soc.,* 77**,** 437-470.

KANE, R. P. 1997. Prediction of Droughts in North-East Brazil: Role of ENSO and Use of Periodicities. *Atmospheric Science Letters,* 17**,** 655-665.

LAT. 1991. *Chance for Peace in Ethiopia:* *http://articles.latimes.com/keyword/president-mengistu-haile-mariam* [Online]. Los Angels Times. [Accessed 5th February 2017].

LIEBMANN, B., HOERLING, M. P., FUNK, C., BLADÉ, I., DOLE, R. M., ALLURED, D., QUAN, X., PEGION, P. & EISCHEID, J. K. 2014. Understanding recent Eastern Horn of Africa rainfall variability and change. *Journal of Climate* 27**,** 8630–8645.

LYON, B. & DEWITT, D. 2012. A recent and abrupt decline in the East African long rains. *Geophys. Res. Lett.,* 39**,** L02702.

MCCABE, G. J. & WOLOCK, D. M. 2015. Variability and trends in global drought. *Earth and Space Science,* 2**,** 223-228.

MCHUGH, M. J. & ROGERS, J. C. 2001. North Atlantic Oscillation Influence on Precipitation Variability around the Southeast African Convergence Zone. *Journal of Climate* 14**,** 3631-3642.

MCKEE, T. B., DOESKEN, N. J. & KLEIST , J. 1993. The Relationship of Drought Frequency and Duration to Time Scales. Proceedings of the Eighth Conference on Applied Climatology. American Meteorological Society: Boston; 179–184.

MPELASOKA, F., HENNESSY, K., JONES, R. & BATES, B. 2008. Comparison of suitable drought indices for climate change impacts assessment over Australia towards resource management. *International Journal of Climatology* 28**,** 1283-1292.

MURPHY, B. F. & TIMBAL, B. 2008. A review of recent climate variability and climate change in southeastern Australia. *International Journal of Climatology, 28, 859-879*.

NCEP. 2017. *Equatorial Pacific Sea Surface Temperatures https://www.ncdc.noaa.gov/teleconnections/enso/indicators/sst.php* [Online]. [Accessed 10 July 2017].

NICHOLSON, E. S. 2014. A detailed look at the recent drought situation in the Greater Horn of Africa *Journal of Arid Environments,* 103**,** 71-79

OSBORN, T. J., BRIFFA, K. R., TETT, S. F. B., JONES, P. D. & TRIGO, R. M. 1999. Evaluation of the North Atlantic oscillation as simulated by a climate model. *Climate Dynamics,* 15,685-702.

OTAKE, M. & PRENTICE, R. L. 1984. The analysis of chromosomally aberrant cells based on beta-binomial distribution. *Radiation Research* 98**,** 456-470.

POZO-V´AZQUEZ, D., ESTEBAN-PARRA, M. J., RODRIGO, F. S. & CASTRO-D´ıEZ, Y. 2000. An analysis of the variability of the North Atlantic oscillation in the time and the frequency domains. *International Journal of Climatology,* 20**,** 1675–1692.

RIDDLE, E. E. & COOK, K. H. 2008. Abrupt rainfall transitions over the Greater Horn of Africa: Observations and regional model simulations. *Journal of Geophysical Research: Atmospheres,* 113**,** D15109.

SAJI, N. H., AMBRIZZI, T. & FERRAZ, S. E. T. 2005. Indian Ocean Dipole Mode events and austral surface air temperature anomalies *Dynamics of Atmospheres and Oceans,* 39**,** 87–10.

SALINGER, M. J., RENWICK, J. A. & MULLAN, A. B. 2001. Interdecadal Pacific Oscillation and South Pacific Climate. *International Journal of Climatology,* 21**,** 1705–1721.

SKLIRIS, N., ZIKA, J. D., NURSER, G., JOSEY, S. A. & MARSH, R. 2016. Global water cycle amplifying at less than the Clausius-Clapeyron rate. Scientific Reports, 6,38752.

SWETNAM, T. W. & BETANCOURT, J. L. 1998. Mesoscale disturbance and ecological response to decadal climatic variability in the American southwest. *Journal of Climate,* 11**,** 3128-3147.

TIERNEY, J. E., UMMENHOFER, C. C. & DEMENOCAL, P. B. 2015. Past and future rainfall in the Horn of Africa. *Science Advances,* 1:e1500682.

UN. 2014. *http://www.un.org/waterforlifedecade/water_and_energy_2014/* [Online]. 2016].

UN. 2017. *http://www.un.org/apps/news/story.asp?NewsID=52578#.WOSH2qFs2po: Drought in Botswana is learning opportunity to achieve water security – UN rights expert* [Online]. [Accessed 5 March 2017].

UNISDR. 2017. *https://www.unisdr.org/archive/52011 :Prolonged drought threatens Greater Horn of Africa* [Online]. United Nations Office for Disaster Risk Reduction. [Accessed 26 March 2017].

VENTON, P. 2012. Drought Risk Management: Practitioners's perspectives from Africa and Asia. UNDP.

WEIL, C. S. 1970. Selection of valid number of sampling units and a consideration of their combination in toxicological studies involving reproduction, teratogenesis or carcinogenesis reproduction, teratogenesis. *Food and Cosmetic Toxicology,* 8**,** 177-182.

WILHITE, D. A., HAYES, M. J., KNUTSON, C. & SMITH, K. H. 2000. Planning for drought: Moving from crisis to risk management. *Journal of the American Water Resources Association, 36,697-710.*

WILLIAMS, A. & FUNK, C. 2011. A westward extension of the warm pool leads to a westward extension of the Walker circulation, drying eastern Africa. *Climate Dynamics,* 37**,** 2417-2435.

WILLIAMS, D. A. 1975. The analysis of binary responses from toxicological experiments involving reproduction and teratogenicity. *Biometrics,* 31**,** 949-952.

WMO 2012. *Standardized Precipitation Index User Guide,* Geneva.

YANG, W., SEAGER, R., CANE, M. A. & B., L. 2014. The East African long rains in observations and models*Journal Climate* 27 7185–7202.